2017

Exploring the Relationship between Nicotinic Acetylcholine Receptor Ligand Size, Efficiency, Efficacy, and C-Loop Opening

Qianyun Ma
Ocean University of China

Han Shen Tae
University of Wollongong, hstae@uow.edu.au

Guanzhao Wu
Ocean University of China, Qingdao National Laboratory for Marine Science and Technology

Tao Jiang
Qingdao National Laboratory for Marine Science and Technology, Ocean University of China

Rilei Yu
Qingdao National Laboratory for Marine Science and Technology, Ocean University of China

Publication Details

Ma, Q., Tae, H., Wu, G., Jiang, T. & Yu, R. (2017). Exploring the Relationship between Nicotinic Acetylcholine Receptor Ligand Size, Efficiency, Efficacy, and C-Loop Opening. Journal of Chemical Information and Modeling, 57 (8), 1947-1956.

Exploring the Relationship between Nicotinic Acetylcholine Receptor Ligand Size, Efficiency, Efficacy, and C-Loop Opening

Abstract
Nicotinic acetylcholine receptors (nAChRs) are ligand-gated ion channels mediating fundamental physiological activities in the nervous system and have become important targets for drug design. For a long time, the acetylcholine binding protein (AChBP) has been used as a surrogate to study the nAChR structure-function. Taking advantage of more than 100 AChBP crystal structures in the Protein DataBank (PDB), we explored the relationship between the size, efficiency, and efficacy of nAChR ligands and the C-loop movement. We found that the size of the ligand is correlated with the opening of the C-loop, which can be used in selecting AChBP crystal structures with appropriate C-loop opening to be used for nAChR ligand docking. Ligand size and C-loop opening are reversely correlated with the ligand efficiency rather than the binding affinity. Ligand efficiency could be accurately predicted using simple computational docking, giving a correlation coefficients (R^2) up to 0.73. The efficacy of nAChR ligands might be related to ligand size, C-loop opening, and ligand efficiency. Results from this study are useful for engineering the binding affinity and efficacy of nAChR ligands.

Disciplines
Medicine and Health Sciences

Publication Details
Ma, Q., Tae, H., Wu, G., Jiang, T. & Yu, R. (2017). Exploring the Relationship between Nicotinic Acetylcholine Receptor Ligand Size, Efficiency, Efficacy, and C-Loop Opening. Journal of Chemical Information and Modeling, 57 (8), 1947-1956.

Exploring the Relationship between Nicotinic Acetylcholine Receptor Ligand Size, Efficiency, Efficacy, and C‑Loop Opening

Qianyun Ma,[†,‡] Han-Shen Tae,[§] Guanzhao Wu,[†,‡] Tao Jiang,[†,‡] and Rilei Yu*[,†,‡]

[†]Key Laboratory of Marine Drugs, Chinese Ministry of Education, School of Medicine and Pharmacy, Ocean University of China,
Qingdao 266003, China
[‡]Laboratory for Marine Drugs and Bioproducts, Qingdao National Laboratory for Marine Science and Technology, Qingdao 266003,
China
[§]Illawarra Health and Medical Research Institute (IHMRI), University of Wollongong, Wollongong, New South Wales 2522,
Australia

INTRODUCTION

Nicotinic acetylcholine receptors (nAChRs) are ligand-gated ion channels involved in fast synaptic transmission and physiological activities in the nervous system.1 nAChRs belong to the cys-loop receptor family, which also includes glycine, serotonin (5-HT3), γ-amino butyric acid type A (GABAA) receptors, and a zinc-activated ion channel.2 There are many different nAChR subtypes with preferential distribution in the nervous system where they mediate different physiological processes.[1] Malfunction of the nAChR is related to neurological disorders such as Parkinson's disease, Alzheimer's disease, schizophrenia, pain, depression, and memory loss.[1,3,4] Hence, nAChRs are important targets for drug design.[1,4] In vertebrates, there are 17 nAChR subunits consisting of α1-α10, β1-β4, γ, δ, and ε. nAChRs are composed of five subunits, with each subunit divided into three domains: an extracellular domain (ECD), a transmembrane domain (TMD), and an intracellular domain (ICD) (Figure 1A,B). The ligand binding site is formed by the ECD of two adjacent subunits (Figure 1C), consisting of loops A, B, and C of the principal subunit and the β-sheet of the complementary subunit. Recently, the published crystal structure of human α4β2 nAChR (PDB code: 5KXI)[5] showed that the agonist, nicotine, is deeply capped into the ligand binding site with the

nicotine positively charged N group oriented to the center of the nAChR aromatic box, forming a cation−π interaction with residue W156. For a long time, the crystal structure of acetylcholine binding protein (AChBP), a homologue of the nAChR ECD, has been used as a template to study nAChR structure and function.[6] Crystal structures of the AChBP in apo, complexed with full agonists, partial agonists, and antagonists, demonstrate that the C-loop of the binding site is very flexible to accommodate the wide spectra of nAChR ligands (Figure 1D,E, Table S1).[7−17] Agonist binding triggers conformational changes in cys-loop receptors, leading to opening of the channel and, consequently, a flux of ions through the channel pore. The starting step for nAChR activation by an agonist is capping of the binding site C-loop into closed conformation.[18−21] The conformational state of the C-loop might be related to the functional state of the nAChR. The ligand binding sites of AChBP are highly plastic, allowing binding of various molecules ranging from small neurotransmitters to large peptide neurotoxins, such as α-conotoxins and snake toxins.[7,17,22] Analysis of the AChBP bound with various ligands of nAChR indicated that the opening of the C-loop bound with full agonist is comparable to or even more closed than that bound with partial agonist, but the latter is remarkably more closed than that bound with antagonist (Figure 1D), in line with the results of Brams et al.[8] It tempts us to assume that a relationship might exists between the conformational states of the C-loop with ligand size, efficiency, and efficacy. In this study, we statistically analyzed 48 crystal structures of AChBP bound with different nAChR ligands (Table S2, Figure S1)[8−17,23−37] to explore the aforementioned relationship between the nAChR ligands and the C-loop.

METHODS

Ligand Size and C-Loop Opening Calculations.

Crystal structures of AChBP bound with nAChR ligands with known binding affinity (PDB ID: 1UV6, 1UW6, 2WNL, 2BYQ, 3WTN, 3WTL, 2BYS, 3WIP, 3U8J, 3ZDG, 4BQT, 3ZDH, 4AFT, 3U8K, 4B5D, 2ZJV, 3C84, 3U8L, 3C79, 3U8M, 2WNC, 2WN9, 3U8N, 2WNJ, 4AFH, 2XNT, 4ALX, 2PGZ, 2XNU, 2XYS, 2W8F, 2W8G, 2X00, 2XYT, 2BYR, 2WZY, 2C9T, 2BR8, 4BFQ, 4DBM, 4QAA, 4QAB, 4QAC, 2Y54, 2Y56, 2Y57, 2Y58 and 1UX2) were selected and downloaded from the Protein DataBank (PDB, http://www.rcsb.org). The number of heavy atoms for the nAChR ligands was calculated using ChemDraw (Figure S1), and the opening of the C-loop of the AChBP was calculated

using Visual Molecular Dynamics (VMD).[38] Ligand Binding Affinity and Ligand Efficiency. The ligand binding affinity (ΔG) was calculated using the equation

$$\Delta G = -RT \ln Kd \quad (1)$$

where R = 8.314 J·mol−1·K−1, T = 300 K, and Kd is the equilibrium dissociation constant.

Ligand efficiency (Δg) was determined using the equation

$$\Delta g = \Delta G / N\text{heavy atoms} \quad (2)$$

where ΔG is the binding free-energy change (or ligand binding affinity) and Nheavy atoms is the number of heavy or non-hydrogen atoms.[39−41]

AutoDock Binding Affinity Calculation.

Structures of AChBP were extracted from PDB entries 1UV6, 1UW6, 2WNL, 2BYQ, 3WTN, 3WTL, 2BYS, 3WIP, 3U8J, 3ZDG, 4BQT, 3ZDH, 4AFT, 3U8K, 4B5D, 2ZJV, 3C84, 3U8L, 3C79, 3U8M, 2WNC, 2WN9, 3U8N, 2WNJ, 4AFH, 2XNT, 4ALX, 2PGZ, 2XNU, 2XYS, 2W8F, 2W8G, 2X00, 2XYT, 2BYR, 2WZY, 2C9T, 2BR8, 4BFQ, 4DBM, 4QAA, 4QAB, 4QAC, 2Y54, 2Y56, 2Y57, 2Y58, 1UX2, 2XZ5, 2YMD, 2YME, 3SH1, 3SIO, 4AFG, 2ZJU, 3WTH, 4UM1, 4UM3, 3WTI, and 3WTJ. Ligands were extracted from the crystal structures, and hydrogen atoms were added. Docking of nAChR ligands to AChBP was performed using AutoDock Tools (ADT)4.2.[42] Gasteiger charges were used, and nonpolar hydrogens of the macromolecule and ligand were merged. A grid box with dimensions of 40 Å × 40 Å × 40 Å and a grid spacing of 0.375 Å was set up and centered on the "aromatic box" between two adjacent subunits of the AChBP. For docking of peptide ligands, a grid box with dimensions of 60 Å × 60 Å × 60 Å was applied. Docking was performed using a Lamarckian genetic algorithm (LGA), with the receptor treated as rigid. The number of LGAs was set using the default values. The produced conformation with minimum binding energy was selected for the analysis.

MOE Binding Affinity Calculation.

Molecular docking was performed using MOE with the AMBER10:EHT force field.[43] AChBP crystal structures used for the ADT calculations above were utilized. The induced fit docking approach was applied with consideration of the side chain flexibility of residues at the binding site. The ligand binding site was defined using the bound ligands in the crystal

structures. Ten docking conformations of the ligands were produced, and the best scored conformation with minimum binding energy was selected for analysis.

MMPBSA Binding Affinity Calculation.

The binding energy calculation module of MMPBSA[44] implemented in AMBER16[45] was used to calculate the binding affinities of the nAChR ligand posed to AChBP using MOE or nAChR ligands in the crystal structures of AChBP. Here, only the minimum energy conformation determined in MOE was used for energy calculation using MMPBSA. Briefly, the internal dielectric and external dielectric constants were set to 2.0 and 80.0, respectively, with a probe radius of 1.4 Å, a grid spacing set to 0.5 Å, and ionic strength set to 0.15 M/L.[46]

RESULTS AND DISCUSSION

All ligands were regularly distributed when they were ranked based on their size and opening of the AChBP C-loop bound with the corresponding ligands. Ligand size could be characterized using the number of heavy atoms (or non-hydrogen atoms), surface area, ligand volume, or molecular weight (Figure S2), among which the number of heavy atoms was most facile to obtain. Here, the number of heavy atoms was selected to represent the ligand size. Ranking nAChR ligands based on their size in order from low to high showed that the full agonists were mostly at the left (low heavy atom number), the antagonists were at the right (high heavy atom number), and the partial agonists were in the middle (Figure 2A, Table S2). Notably, the distribution boundary between the partial agonists and antagonists is not clearly defined. Indeed, some of the nAChR ligands are antagonists despite their comparable or smaller size than that of the partial agonists.[15–17] Interestingly, these ligands are rich of aromatic rings that could appropriately orient their position to form π–π stacking interactions with the aromatic residues of the binding site, and the C-loop was usually stabilized in an open conformation (Figure S3).

Similarly, using the distance of the C-loop opening as the ranking parameter of the ligands (from smallest to largest shift), the agonists had the least and modest impact on the C-loop movement, respectively. The antagonists, however, resulted in the largest shift of the C-loop opening (Figure 2B, Table S2). However, unlike the ligand size distribution profile, the boundary between the agonists and antagonists is more clearly defined. Thus, C-loop opening

measurement is a more reliable indicator to differentiate the agonists from the antagonists of the nAChR.

The correlation between the C-loop shift and nAChR agonist efficacy though, is unclear (Figure 2B). Indeed, there remains controversy over the correlation between the opening of the C-loop and agonist efficacy of the nAChR.[8,24,37] It is challenging to use the limited number of AChBP crystal structures to thoroughly understand the structure−function relationships of nAChR agonists. The AChBP crystal structure is homologus to the ECD of nAChR, and therefore, the conformational state of the C-loop on AChBP might not be exactly the same to that of the nAChR as trivial differences exist.[47,48] In addition, nAChR agonists can behave differently at different nAChR subtypes. For instance, nicotine activates other subtypes of nAChR while antagonizing the α9α10 nAChR subtype.[49,50] In addition, choline is a known α7 nAChR subtype-selective agonist but acts as a partial agonist for some other nAChR subtypes.[51] The ligand efficacy of the nAChR is related to not only the ligand binding and the induced conformation perturbation at the binding site but also the gating processes of the receptor. Overall, the opening of the C-loop is correlated with the ligand size of nAChR, with a correlation coefficient (R2) of 0.54 (Figure 2C). Exclusion of five ligands (in the dashed frame of Figure 2C) with distinctive structure or unusual binding manner (Figure S3) from the analysis improved the R2 value to 0.86 (Figure 2D). These five ligands are relatively small, but they are rich in aromatic rings. These rings are often linked through flexible rational bonds, and they can adjust their conformation to play a role of supporter (Figure S3A−D) or they can form π−π stacking interactions with each other to produce a "ligand cluster" (Figure S3E). The C-loop of the binding site is very flexible, thus allowing it to adjust its conformation or opening to accommodate various nAChR ligands of different sizes (Figure 3). Therefore, it is not surprising to observe the correlation between the ligand size and C-loop opening induced by the corresponding ligands. However, it has to be noted that ligands, usually antagonists of the nAChRs, with distinctive structure or unusual binding manner (Figure S3) can still stabilize the open conformation of the C-loop by forming π−π stacking interactions with aromatic residues of the binding site despite their relatively small size in comparison to the partial agonists (Figure S3, Table S2). As a result, there is not clear distinction between the partial agonists and antagonists with distinctive structure or unusual binding manner when they are ranked based on the size. Nevertheless, in general, there is good agreement between the size of the ligand and the opening of the C-loop, which can be

predicted using the ligand size as the input variable. As shown in Figure 2D, the opening of the C-loop (Å) can be predicted using eq 3

$$f(x) = 0.11x + 8.9$$

$$(n = 43, R^2 = 0.86, \text{SD} = 2.33, q^2 = 10.88, F = 247.159) \quad (3)$$

where x is the number of heavy atoms.

To date, over 100 crystal structures of AChBP bound with different nAChRs ligands are available in the PDB, providing sufficient models of the C-loop movement to understand the ligand nAChR structure−activity relationship.[16,52] Correct selection of the crystal structures is essential for accurate docking models of nAChR ligands. Here, we proposed the use of eq 3 in selecting suitable ligand-bound AChBP crystal structures for generation of docking models. To evaluate the accuracy of eq 3 in predicting the opening of the C-loop of AChBP, we randomly chose four nAChR ligands (Table 1) with known AChBP-bound crystal structures from the PDB[22,52−54] and compared the calculated opening of the Cloop for each ligand using eq 3 with their respective crystal structures. For the four ligands, the calculated values of the C-loop opening are similar to the values determined from ligand-bound crystal structures, with 2−3 Å deviation (Table 1).

Crystal structures of AChBP with a C-loop opening close to our predicted values were then selected for nAChR ligand docking. Docking studies suggested that the binding modes of the four nAChR ligands can be correctly predicted using the selected AChBP crystal structures (Figure 4) with a root-mean-square deviation (RMSD) of less than 2 Å. In contrast, the binding orientation of these ligands significantly deviated from their respective crystal structures (RMSD > 3 Å) when AChBP structures with a substantially open or closed C-loop were used for docking (Figure S4). Thus, the conformational state of the C-loop and selection of the correct crystal structures for nAChR molecular docking or as a homology modeling template should be considered in future modeling studies of the nAChR ligands.

Ranking of the ligands based on their binding affinity resulted in irregular distribution (Figure 5A, Table S2). In contrast, using the binding efficiency of the agonists and antagonists as the ranking parameter, most of the full agonists had the highest binding efficiency followed by the partial agonists and the antagonists with the lowest efficiency (Figure 5B, Table S2). Thus, the binding efficiency of the ligands rather than their binding affinities could be used to differentiate the agonists from the antagonists of the nAChR.

Our analysis also indicated that no correlation was found between ligand size and binding affinity (R^2 = 0.05) (Figure 5C), whereas a strong linear correlation was identified (R^2 = 0.7) between the logarithm of the number of the heavy atoms (or ligand size) and ligand efficiency (Figure 5D). Indeed, comparison of protein−ligand binding affinities for over 8000 ligands with 28 protein targets shows that the ligand efficiency rather than average ligand binding affinities is correlated with molecular size.[55] Large ligands usually form more contacts with the receptor than smaller size ligands, whereas the binding affinities of the former do not overwhelm that of the latter (Figure 5A, Table S2). Thus, it is not rational to improve the binding affinity of the nAChR ligands merely by increasing the ligand size. Instead, optimization of their structure and functional groups might be a more feasible choice. In contrast, ligand efficiency is reversely correlated with the logarithm of ligand size in a linear way. Therefore, ligand size should be considered as the priority when the ligand efficiency of the nAChR ligands are modified in future drug design.

Comparison of the ligand binding affinity with the opening of the C-loop suggested that there was no correlation (R^2 = 0.00048) (Figure 5E). The ligand efficiency, however, is well reversely correlated with the opening of the C-loop (R^2 = 0.53) (Figure 5F). nAChR ligands with higher efficiency tend to cap the C-loop into a more closed conformation and vice versa, in line with the observations that full and partial agonists tend to capture the conformation of the C-loop in fully and partially closed states, respectively. In comparison, the antagonists mostly stabilize the C-loop of the nAChR into an open conformation (Figure 2B).[8,24]

Ligand efficiency, simply defined as ligand binding in terms of free energy per heavy atom,[39,40] could be useful in deciding the potential further optimization of particular “hits” and chemical scaffolds. The efficacy of a ligand, on the other hand, is generally determined by the ligand’s ability to promote a quantifiable biological response upon binding.[56] We found that there might be some correlation between ligand efficiency and ligand efficacy for nAChR ligands (Figure 5B). In comparison to ligand size, ligand efficiency might be a more reliable indicator to differentiate the agonists from the antagonists of the nAChR as ligand efficiency takes into account the size and binding affinity of the ligand (Equation 2). Indeed, a small size ligand with very poor binding affinity cannot function as a full agonist, until it binds to the nAChR and caps the C-loop into the closed conformation.

Interestingly, we found that ligand efficiencies could be simply predicted using computational docking.[8−17,23−37,57−60] As shown in Figure 6A,B, the predicted ligand

efficiencies using MOE and ADT are well correlated with the experimentally determined ligand efficiencies (R^2 = 0.57 and 0.73, respectively) (Figure S5). We also evaluated the performance of MMPBSA at predicting ligand efficiency, and we found that its performance is comparable to ADT but a little inferior to MOE (Figure 6C,D and Figure S6). Overall, the ligand efficiency could be well predicted using molecular docking, an extremely fast and economical binding affinity calculation method.

CONCLUSIONS

In this study, we statistically analyzed 48 crystal structures of the AChBP bound with different nAChR ligands with known binding affinities to explore the relationship between nAChR ligand size, efficiency, and efficacy and C-loop opening. We found that the opening of the C-loop of the crystal structure of AChBP is correlated with the ligand size except for a few ligands with distinctive structure or with unusual binding modes. For a given ligand, the opening of the bound C-loop could be predicted based on an equation derived from statistical analysis of 43 nAChR ligands bound to the crystal structures of AChBP. Crystal structures of the AChBP with C-loop opening most close to the calculated values were selected for nAChR ligand docking, and the predicted pose of the ligand is well superimposed with that determined in the crystal structure. Additionally, we found that ligand efficiency rather than affinity was correlated with the size of the ligand and C-loop opening, and ligand efficiency could be predicted using the computational docking method. Full agonists, partial agonists, and antagonists of the nAChR were regularly distributed in major when they were ranked based on their size, C-loop opening, or the ligand efficiency. Ligand size, C-loop opening, and ligand efficiency might have certain amplitudes of correlations with the ligand efficacy, and they are implicated to be useful to distinguish the agonists and antagonists of the nAChR.

In summary, establishing the relationship between ligand size, C-loop opening, ligand efficiency, and ligand efficacy is important for not only accurate prediction of the binding modes of the nAChR ligands but also in differentiation of the agonists from the antagonists of the nAChR. As the number of AChBP crystal structures bound with different nAChR ligands continues to increase, it will give rise to more accurate knowledge-based computational methods for rational design of ligands targeting the cys-loop receptors.

ASSOCIATED CONTENT

*S Supporting Information

The Supporting Information is available free of charge on the ACS Publications website at DOI: 10.1021/acs.jcim.7b00152.

Structures of the ligands, correlation plots, binding images, (PDF)

Statistics of the crystal structures, crystal structure parameters, size parameters, ligand binding parameters, (XLSX)

Calculated energies (XLSX)

AUTHOR INFORMATION

Corresponding Author

*E-mail: ryu@ouc.edu.cn. Tel: 0086-532-82031615. Fax: 0086-532-82033054. Address: School of Medicine and Pharmacy, Ocean University of China, 5 Yushan Road, Qingdao 266003, China.

ORCID

Tao Jiang: 0000-0002-6590-5041

Rilei Yu: 0000-0001-6625-2014

Notes

The authors declare no competing financial interest.

ACKNOWLEDGMENTS

This work was supported by the Fundamental Research Funds for the Central Universities, China Postdoctoral Science Foundation grant (2016T90655), Special Foundation for Qingdao Basic Research Program (15-9-1-85-jch), and the Scientific and Technological Innovation Project financially supported by Qingdao National Laboratory for Marine Science and Technology (No. 2015ASKJ02). The authors gratefully acknowledge funding from the above sources.

REFERENCES

(1) Taly, A.; Corringer, P.-J.; Guedin, D.; Lestage, P.; Changeux, J.-P. Nicotinic Receptors: Allosteric Transitions and Therapeutic Targets in the Nervous System. *Nat. Rev. Drug Discov.***2009**, *8*, 733–750.

(2) Lester, H. A.; Dibas, M. I.; Dahan, D. S.; Leite, J. F.; Dougherty, D. A. Cys-Loop Receptors: New Twists and Turns. *Trends Neurosci.***2004**, *27*, 329–336.

(3) Levin, E. D.; Rezvani, A. H. Nicotinic Interactions with Antipsychotic Drugs, Models of Schizophrenia and Impacts on Cognitive Function. *Biochem. Pharmacol.***2007**, *74*, 1182–1191.

(4) Arneric, S. P.; Holladay, M.; Williams, M. Neuronal Nicotinic Receptors: A Perspective on Two Decades of Drug Discovery Research. *Biochem. Pharmacol.***2007**, *74*, 1092–1101.

(5) Morales-Perez, C. L.; Noviello, C. M.; Hibbs, R. E. X-Ray Structure of the Human α4β2 Nicotinic Receptor. *Nature.***2016**, *538*, 411–415.

(6) Brejc, K.; van Dijk, W. J.; Klaassen, R. V.; Schuurmans, M.; van Der Oost, J.; Smit, A. B.; Sixma, T. K. Crystal Structure of an ACh-Binding Protein Reveals the Ligand-Binding Domain of Nicotinic Receptors. *Nature.***2001**, *411*, 269–276.

(7) Hansen, S. B.; Sulzenbacher, G.; Huxford, T.; Marchot, P.; Taylor, P.; Bourne, Y. Structures of AplysiaAChBP Complexes with Nicotinic Agonists and Antagonists Reveal Distinctive Binding Interfaces and Conformations. *EMBO J.***2005**, *24*, 3635–3646.

(8) Brams, M.; Pandya, A.; Kuzmin, D.; van Elk, R.; Krijnen, L.; Yakel, J. L.; Tsetlin, V.; Smit, A. B.; Ulens, C. A Structural and Mutagenic Blueprint for Molecular Recognition of Strychnine and D-Tubocurarine by Different Cys-Loop Receptors.*PLoS Biol.***2011**, *9*, e1001034.

(9) Celie, P. H., van Rossum-Fikkert, S. E., van Dijk, W. J., Brejc, K., Smit, A. B., &Sixma, T. K. Nicotine and carbamylcholine binding to nicotinic acetylcholine receptors as studied in AChBP crystal structures. *Neuron.***2004**,*41*, 907-914.

(10) Hansen, S. B., Sulzenbacher, G., Huxford, T., Marchot, P., Taylor, P., & Bourne, Y. Structures of AplysiaAChBP complexes with nicotinic agonists and antagonists reveal distinctive binding interfaces and conformations. *The EMBO journal.***2005**, *24*, 3635-3646.

(11) Ihara M, Okajima T, Yamashita A, Oda T, Asano T, Matsui M, Sattelle D, andMatsuda K. Studies on an acetylcholine binding protein identify a basic residue in loop G on the β1 strand as a new structural determinant of neonicotinoid actions. *Molecular pharmacology.***2014**, *86*, 736-746.

(12) Olsen, J. A., Balle, T., Gajhede, M., Ahring, P. K., &Kastrup, J. S. Molecular recognition of the neurotransmitter acetylcholine by an acetylcholine binding protein reveals determinants of binding to nicotinic acetylcholine receptors. *PloS one.***2014**, *9*, e91232.

(13) Rohde, L. A. H.; Ahring, P. K.; Jensen, M. L.; Nielsen, E. Ø.; Peters, D.; Helgstrand, C.; Krintel, C.;Harpsøe, K.; Gajhede, M.; Kastrup, J. S. Intersubunit bridge formation governs agonist efficacy at nicotinic acetylcholine α4β2 receptors: unique role of halogen bonding revealed. *J. Biol. Chem.***2012,** 287, 4248-4259.

(14) Rucktooa, P., Haseler, C. A., van Elk, R., Smit, A. B., Gallagher, T., &Sixma, T. K. Structural characterization of binding mode of smoking cessation drugs to nicotinic acetylcholine receptors through study of ligand complexes with acetylcholine-binding protein. *J. Biol. Chem.* **2012**, *287*, 23283-23293.

(15) Akdemir, A.; Rucktooa, P.; Jongejan, A.; Elk, R. van; Bertrand, S.; Sixma, T. K.; Bertrand, D.; Smit, A. B.; Leurs, R.; de Graaf, C.; de Esch, I. J. P. Acetylcholine

Binding Protein (AChBP) as Template for Hierarchical in Silico Screening Procedures to Identify Structurally Novel Ligands for the Nicotinic Receptors. *Bioorg. Med. Chem.* **2011**,*19*, 6107–6119.

(16) Ulens, C.; Akdemir, A.; Jongejan, A.; van Elk, R.; Bertrand, S.; Perrakis, A.; Leurs, R.; Smit, A. B.; Sixma, T. K.; Bertrand, D.; de Esch, I. J. P. Use of Acetylcholine Binding Protein in the Search for Novel α7 Nicotinic Receptor Ligands. In Silico Docking, Pharmacological Screening, and X-Ray Analysis.*J. Med. Chem.***2009**, *52*, 2372–2383.

(17) Ulens, C., Hogg, R. C., Celie, P. H., Bertrand, D., Tsetlin, V., Smit, A. B., &Sixma, T. K. Structural determinants of selective α-conotoxin binding to a nicotinic acetylcholine receptor homolog AchBP. *Proc. Natl. Acad. Sci. U S A* **2006**,*103*, 3615-3620.

(18) Cheng, X.; Wang, H.; Grant, B.; Sine, S. M.; McCammon, J. A. Targeted Molecular Dynamics Study of C-Loop Closure and Channel Gating in Nicotinic Receptors. *Plos.Comput.Biol.***2006**, *2*, e134.

(19) Gao, F.; Bren, N.; Burghardt, T. P.; Hansen, S.; Henchman, R. H.; Taylor, P.; McCammon, J. A.; Sine, S. M. Agonist-Mediated Conformational Changes in Acetylcholine-Binding Protein Revealed by Simulation and Intrinsic Tryptophan Fluorescence. *J. Biol. Chem.***2005**, *280*, 8443–8451.

(20) Absalom, N. L.; Lewis, T. M.; Schofield, P. R. Mechanisms of Channel Gating of the Ligand-Gated Ion Channel Superfamily Inferred from Protein Structure. *Exp. Physiol.***2004**, *89*, 145–153.

(21) Purohit, P.; Auerbach, A. Loop C and the Mechanism of Acetylcholine Receptor-Channel Gating. *J. Gen. Physiol.***2013**, *141*, 467–478.

(22) Bourne, Y.; Talley, T. T.; Hansen, S. B.; Taylor, P.; Marchot, P. Crystal Structure of a Cbtx-AChBP Complex Reveals Essential Interactions between Snake Alpha-Neurotoxins and Nicotinic Receptors. *EMBO.J.***2005**, *24*, 1512–1522.

(23) Stornaiuolo, M.; De Kloe, G. E.; Rucktooa, P.; Fish, A.; van Elk, R.; Edink, E. S.; Bertrand, D.; Smit, A. B.; de Esch, I. J. P.; Sixma, T. K. Assembly of a π–π Stack of Ligands in the Binding Site of an Acetylcholine-Binding Protein. *Nat. Commun.***2013**, *4*, 1875.

(24) Hibbs, R. E.; Sulzenbacher, G.; Shi, J.; Talley, T. T.; Conrod, S.; Kem, W. R.; Taylor, P.; Marchot, P.; Bourne, Y. Structural Determinants for Interaction of Partial Agonists with Acetylcholine Binding Protein and Neuronal α7 Nicotinic Acetylcholine Receptor. *EMBO. J.***2009**, *28*, 3040–3051.

(25) Celie, P. H.; Kasheverov, I. E.; Mordvintsev, D. Y.; Hogg, R. C.; van Nierop, P.; van Elk, R.; van Rossum-Fikkert, S. E.; Zhmak, M. N.; Bertrand, D.; Tsetlin, V. Crystal structure of nicotinic acetylcholine receptor homolog AChBP in complex with an α-conotoxinPnIA variant. *Nat.Struct. Mol. Biol.***2005,** 12, 582-588.

(26) Hansen S B, Taylor P. Galanthamine and non-competitive inhibitor binding to ACh-binding protein: evidence for a binding site on non-α-subunit interfaces of heteromeric neuronal nicotinic receptors. *J. Mol. Biol.***2007**, *369*, 895-901.

(27) Bourne, Y.; Radić, Z.; Aráoz, R.; Talley, T. T.; Benoit, E.; Servent, D.; Taylor, P.; Molgó, J.; Marchot, P. Structural determinants in phycotoxins and AChBP conferring high affinity binding and nicotinic AChR antagonism. *Proc. Natl. Acad. Sci. U S A.***2010,** 107, 6076-6081.

(28) Edink, E.; Rucktooa, P.; Retra, K.; Akdemir, A.; Nahar, T.; Zuiderveld, O.; van Elk, R.; Janssen, E.; van Nierop, P.; van Muijlwijk-Koezen, J. Fragment growing induces conformational changes in acetylcholine-binding protein: a structural and thermodynamic analysis. *J. Am. Chem. Soc.***2011,** 133, 5363-5371.

(29) Ihara, M.; Okajima, T.; Yamashita, A.; Oda, T.; Hirata, K.; Nishiwaki, H.; Morimoto, T.; Akamatsu, M.; Ashikawa, Y.; Kuroda, S. Crystal structures of

LymnaeastagnalisAChBP in complex with neonicotinoid insecticides imidacloprid and clothianidin. *Invert. Neurosci.***2008,** 8, 71-81.

(30) Talley, T. T., Harel, M., Hibbs, R. E., Radić, Z., Tomizawa, M., Casida, J. E., & Taylor, P. Atomic interactions of neonicotinoid agonists with AChBP: molecular recognition of the distinctive electronegative pharmacophore. *Proc. Natl. Acad. Sci. U S A.***2008**,*105*, 7606-7611.

(31) Ussing, C. A.; Hansen, C. P.; Petersen, J. G.; Jensen, A. A.; Rohde, L. A.; Ahring, P. K.; Nielsen, E. Ø.; Kastrup, J. S.; Gajhede, M.; Frølund, B. Synthesis, pharmacology, and biostructural characterization of novel α4β2 nicotinic acetylcholine receptor agonists. *J. Med. Chem.***2013,** 56, 940-951.

(32) Billen, B.; Spurny, R.; Brams, M.; van Elk, R.; Valera-Kummer, S.; Yakel, J. L.; Voets, T.; Bertrand, D.; Smit, A. B.; Ulens, C. Molecular actions of smoking cessation drugs at α4β2 nicotinic receptors defined in crystal structures of a homologous binding protein. *Proc. Natl. Acad. Sci. U S A.***2012,** 109, 9173-9178.

(33) Shahsavar, A., Kastrup, J. S., Nielsen, E. Ø., Kristensen, J. L., Gajhede, M., &Balle, T. Crystal structure of LymnaeastagnalisAChBP complexed with the potent nAChR antagonist DH β E suggests a unique mode of antagonism. *PLoS. One.***2012**,*7*, e40757.

(34) Zhang, H.; Eaton, J. B.; Yu, L.; Nys, M.; Mazzolari, A.; Van Elk, R.; Smit, A. B.; Alexandrov, V.; Hanania, T.; Sabath, E. Insights into the structural determinants required for high-affinity binding of chiral cyclopropane-containing ligands to α4β2-nicotinic acetylcholine receptors: an integrated approach to behaviorally active nicotinic ligands. *J. Med. Chem.* **2012,** 55, 8028-8037.

(35) Grimster, N. P.; Stump, B.; Fotsing, J. R.; Weide, T.; Talley, T. T.; Yamauchi, J. G.; Nemecz, Á.; Kim, C.; Ho, K.; Sharpless, K. B. Generation of candidate ligands for nicotinic acetylcholine receptors via in situ click chemistry with a soluble acetylcholine binding protein template. *J. Am. Chem. Soc.***2012,** 134, 6732-6740.

(36) Kaczanowska, K., Harel, M., Radić, Z., Changeux, J. P., Finn, M. G., & Taylor, P. Structural basis for cooperative interactions of substituted 2-aminopyrimidines with the acetylcholine binding protein. *Proc. Natl. Acad. Sci. U S A.***2014**,*111*, 10749-10754.

(37) Rohde, L. A. H.; Ahring, P. K.; Jensen, M. L.; Nielsen, E. Ø.; Peters, D.; Helgstrand, C.; Krintel, C.; Harpsøe, K.; Gajhede, M.; Kastrup, J. S.; Balle, T. Intersubunit Bridge Formation Governs Agonist Efficacy at Nicotinic Acetylcholine α4β2 Receptors: Unique Role of Halogen Bonding Revealed. *J. Biol. Chem.***2012**, *287*, 4248–4259.

(38) Humphrey, W.; Dalke, A.; Schulten, K. VMD: Visual Molecular Dynamics. *J. Mol. Graph.***1996**, *14*, 33–38, 27–28.

(39) Andrews, P. R.; Craik, D. J.; Martin, J. L. Functional Group Contributions to Drug-Receptor Interactions. *J. Med. Chem.***1984**, *27*, 1648–1657.

(40) Kuntz, I. D.; Chen, K.; Sharp, K. A.; Kollman, P. A. The Maximal Affinity of Ligands.*Proc. Natl. Acad. Sci. U. S. A.***1999**, *96*, 9997–10002.

(41) Hopkins, A. L.; Groom, C. R.; Alex, A. Ligand Efficiency: A Useful Metric for Lead Selection. *Drug.Discov.Today.* **2004**, *9*, 430–431.

(42) Morris, G. M.; Huey, R.; Lindstrom, W.; Sanner, M. F.; Belew, R. K.; Goodsell, D. S.; Olson, A. J. AutoDock4 and AutoDockTools4: Automated Docking with Selective Receptor Flexibility. *J. Comput. Chem.***2009**, *30*, 2785–2791.

(43) Vilar, S.; Cozza, G.; Moro, S. Medicinal Chemistry and the Molecular Operating Environment (MOE): Application of QSAR and Molecular Docking to Drug Discovery. *Curr.Top. Med. Chem.***2008**, *8*, 1555–1572.

(44) Miller, B. R.; McGee, T. D.; Swails, J. M.; Homeyer, N.; Gohlke, H.; Roitberg, A. E. MMPBSA.py: An Efficient Program for End-State Free Energy Calculations. *J. Chem. Theory. Comput.***2012**, *8*, 3314–3321.

(45) D.A. Case, R.M. Betz, W. Botello-Smith, D.S. Cerutti, T.E. Cheatham, III, T.A. Darden, R.E. Duke, T.J. Giese, H. Gohlke, A.W. Goetz, N. Homeyer, S. Izadi, P. Janowski, J. Kaus, A. Kovalenko, T.S. Lee, S. LeGrand, P. Li, C. Lin, T. Luchko, R. Luo, B. Madej, D. Mermelstein, K.M. Merz, G. Monard, H. Nguyen, H.T. Nguyen, I. Omelyan, A. Onufriev, D.R. Roe, A. Roitberg, C. Sagui, C.L. Simmerling, J. Swails, R.C. Walker, J. Wang, R.M. Wolf, X. Wu, L. Xiao, D.M. York and P.A. Kollman , AMBER 2016, University of California, San Francisco.

(46) Yu, R.; Craik, D. J.; Kaas, Q. Blockade of Neuronal α7-nAChR by α-ConotoxinImI Explained by Computational Scanning and Energy Calculations. *PLoSComput.Biol.***2011**, *7*, e1002011.

(47) Zouridakis, M., Giastas, P., Zarkadas, E., Chroni-Tzartou, D., Bregestovski, P., &Tzartos, S. J. Crystal structures of free and antagonist-bound states of human α9 nicotinic receptor extracellular domain. *Nat.Struct. Mol. Biol.***2014**,*21*, 976-980.

(48) Dellisanti, C. D., Yao, Y., Stroud, J. C., Wang, Z. Z., & Chen, L. Crystal structure of the extracellular domain of nAChR α1 bound to α-bungarotoxin at 1.94 Å resolution. *Nat. Neurosc.***2007**,*10*, 953-962.

(49) Elgoyhen, A. B., Johnson, D. S., Boulter, J., Vetter, D. E., & Heinemann, S. α9: an acetylcholine receptor with novel pharmacological properties expressed in rat cochlear hair cells. *Cell.***1994**,*79*, 705-715.

(50) Elgoyhen, A. B., Vetter, D. E., Katz, E., Rothlin, C. V., Heinemann, S. F., & Boulter, J. α10: a determinant of nicotinic cholinergic receptor function in mammalian vestibular and cochlear mechanosensory hair cells.*Proc. Natl. Acad. Sci. U S A.* **2001**,*98*, 3501-3506.

(51) Sgard, F.; Charpantier, E.; Bertrand, S.; Walker, N.; Caput, D.; Graham, D.; Bertrand, D.; Besnard, F. A novel human nicotinic receptor subunit, α10, that confers functionality to the α9-subunit. *Mol.Pharmacol.* **2002,** 61, 150-159.

(52) Dutertre, S.; Ulens, C.; Büttner, R.; Fish, A.; van Elk, R.; Kendel, Y.; Hopping, G.; Alewood, P. F.; Schroeder, C.; Nicke, A.; Smit, A. B.; Sixma, T. K.; Lewis, R. J. AChBP-Targeted Alpha-Conotoxin Correlates Distinct Binding Orientations with nAChR Subtype Selectivity. *EMBO. J.***2007**, *26*, 3858–3867.

(53) Luo, J.; Taylor, P.; Losen, M.; de Baets, M. H.; Shelton, G. D.; Lindstrom, J. Main Immunogenic Region Structure Promotes Binding of Conformation-Dependent Myasthenia Gravis Autoantibodies, Nicotinic Acetylcholine Receptor Conformation Maturation, and Agonist Sensitivity. *J. Neurosci.***2009**, *29*, 13898–13908.

(54) Bourne, Y.; Sulzenbacher, G.; Radiæ, Z.; Aráoz, R.; Reynaud, M.; Benoit, E.; Zakarian, A.; Servent, D.; Molgó, J.; Taylor, P.; Marchot, P. Marine Macrocyclic Imines, Pinnatoxins A and G: Structural Determinants and Functional Properties to Distinguish Neuronal α7 from Muscle α12βγδnAChRs. *Struct.Lond. Engl.* **2015**, *23*, 1106–1115.

(55) Reynolds, C. H.; Bembenek, S. D.; Tounge, B. A. The Role of Molecular Size in Ligand Efficiency.*Bioorg. Med. Chem. Lett.***2007**, *17*, 4258–4261.

(56) Galandrin, S.; Oligny-Longpré, G.; Bouvier, M. The Evasive Nature of Drug Efficacy:

Implications for Drug Discovery. *Trends.Pharmacol. Sci.***2007**, *28*, 423–430.

(57) Brams, M.; Gay, E. A.; Sáez, J. C.; Guskov, A.; van Elk, R.; van der Schors, R. C.; Peigneur, S.; Tytgat, J.; Strelkov, S. V.; Smit, A. B. Crystal structures of a cysteine-modified mutant in loop D of acetylcholine-binding protein. *J. Biol. Chem.***2011,** 286, 4420-4428.

(58) Kesters, D.; Thompson, A. J.; Brams, M.; Van Elk, R.; Spurny, R.; Geitmann, M.; Villalgordo, J. M.; Guskov, A.; Danielson, U. H.; Lummis, S. C. Structural basis of ligand recognition in 5 - HT3 receptors. *EMBO. Rep.***2013**,*14*, 49-56.

(59) Nemecz Á, Taylor P. Creating an α7 nicotinic acetylcholine recognition domain from the acetylcholine-binding protein: crystallographic and ligand selectivity analyses. *J. Biol. Chem.* **2011**, *286*,42555-42565.

(60) Shahsavar, A., Ahring, P. K., Olsen, J. A., Krintel, C., Kastrup, J. S., Balle, T., &Gajhede, M. Acetylcholine-binding protein engineered to mimic the α4-α4 binding pocket in α4β2 nicotinic acetylcholine receptors reveals interface specific interactions important for binding and activity. *Mol. Pharmacol.***2015**,*88*, 697-707.

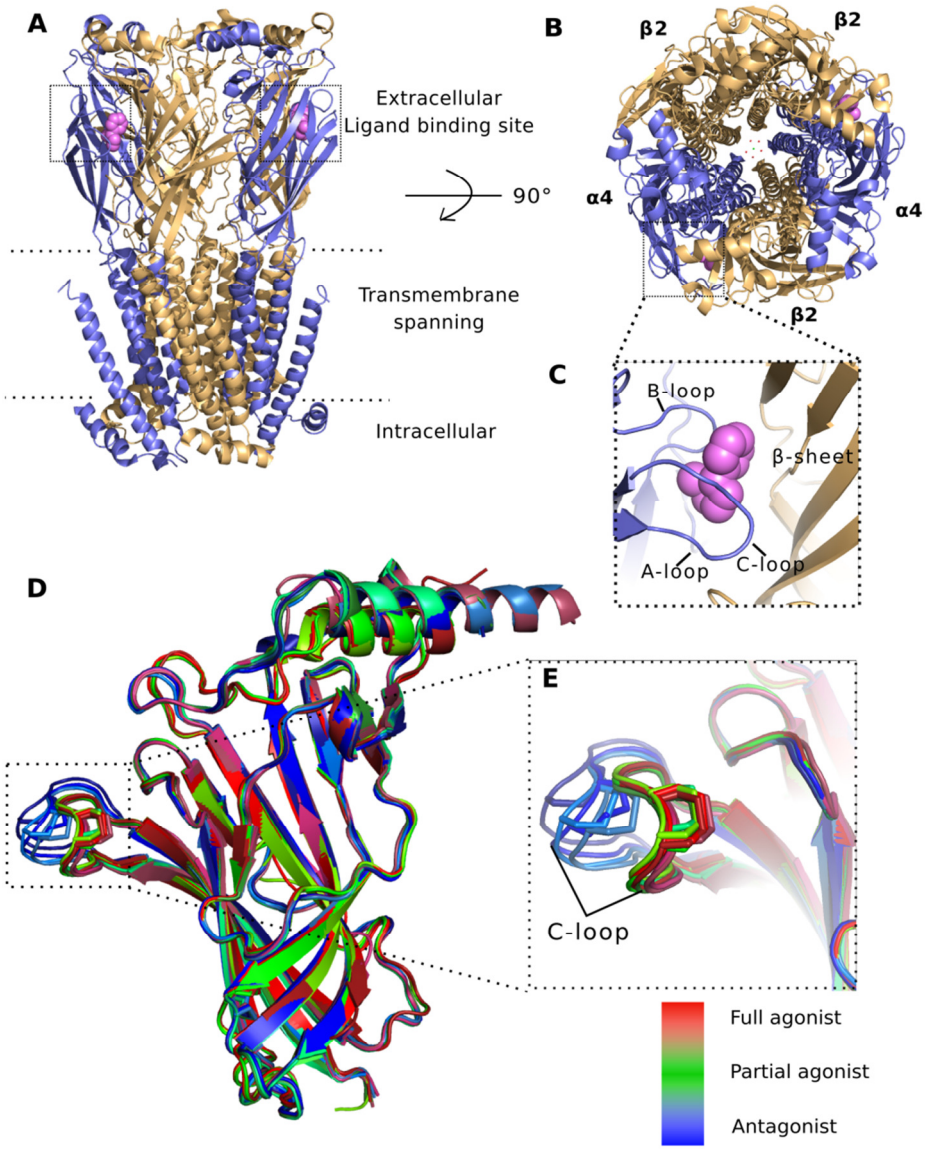

Figure 1. Crystal structures of human α4β2 nAChR (PDB ID: 5KXI) with bound nicotine molecules and AChBPs (PDB ID: 1UV6, 2BYS, 2BYQ, 3WTN, 3WIP, 3U8J, 4BQT, 4AFT, 2XNT, 2W8F, 2BYR, 2C9T). (A) Side view of the human α4β2 nAChR with two nicotine molecules (magenta) bound to the ECD binding site (dashed frame). The α4 and β2 subunits are colored blue and gold, respectively. (B) Top view of the human α4β2 nAChR, with (C) the ligand binding site magnified (dashed frame). The ligand binding site is comprised of loops A, B, and C of the α4 (principal) subunit and β-sheet of the β4 (complementary) subunit. (D) Superimposed crystal structures of full agonist (red) (PDB ID: 1UV6, 2BYS, 2BYQ, 3WTN, 3WIP), partial agonist (green) (PDB ID: 3U8J, 4BQT, 4AFT), and antagonist (blue) (PDB ID: 2XNT, 2W8F, 2BYR, 2C9T) bound- AChBP, with the C-loop highlighted

(dashed frame). For clarity, only one AChBP subunit is shown. (E) Magnification of the ligand-bound AChBP C-loop.

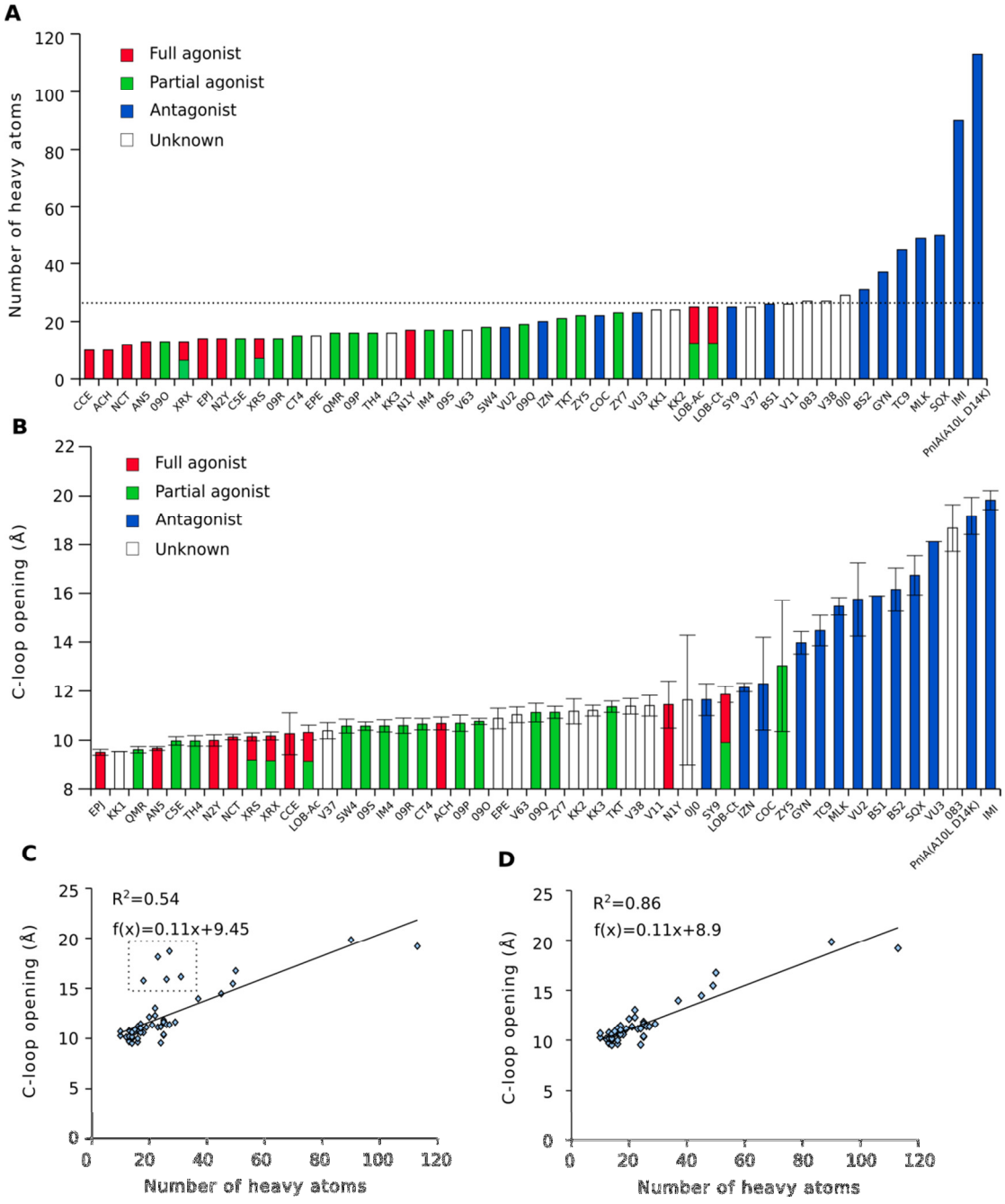

Figure 2. Correlation between nAChR ligand size and C-loop opening. (A) Size-based ranking of nAChR full agonists (red), partial agonists (green), antagonists (blue), and ligands with unknown property (white) in order from small to large. (B) Distribution of the opening of the C-loop bound with full agonists (red), partial agonists (green), antagonists (blue), and ligands with unknown property (white) in order from minimum to maximum (mean ± SEM, n = 5). Then AChR ligand size and C-loop opening correlation coefficient score (R^2) for (C) all ligands is 0.54, and (D) that after removal of ligands with special binding profiles (dashed frame from C) is 0.86.

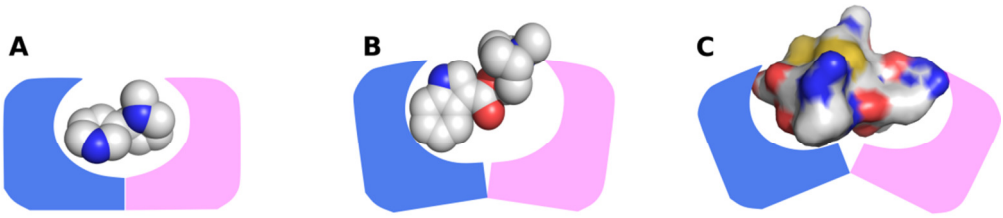

Figure 3. Schematic profile of ligand-bound nAChR. (A) Full agonist (nicotine), (B) partial agonist (Tropisetron), and (C) antagonist (α-conotoxin ImI) binding to the nAChR ligand binding site. The binding site is formed by the principal (blue) and complementary (magenta) interfaces of two adjacent subunits.

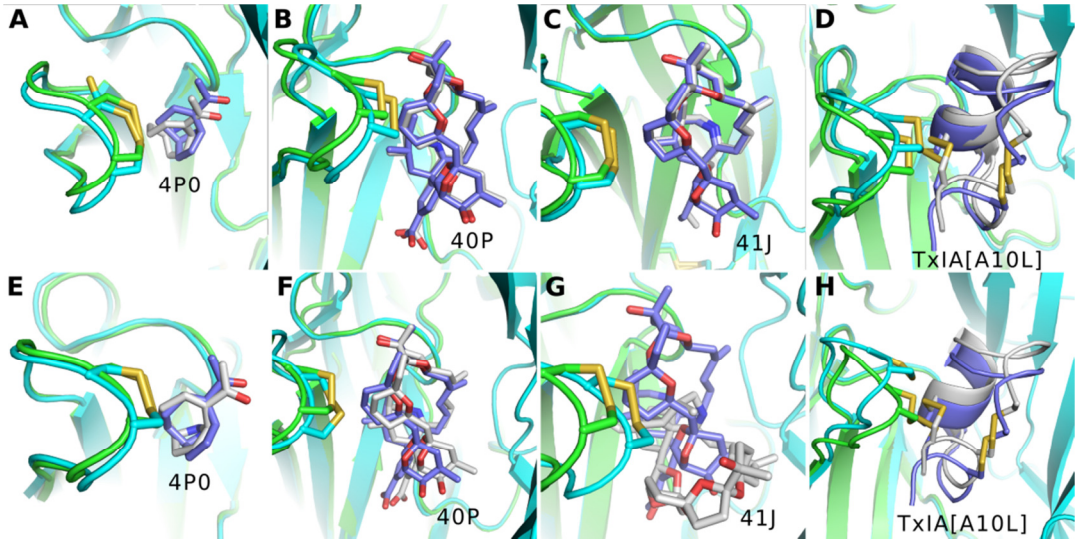

Figure 4. Comparison of computationally determined binding of nAChR ligands (gray) to AChBP (cyan) with crystallographically determined binding of the same ligands (purple-blue) to AChBP (green). Two ligand-bound AChBP crystal structures with a C-loop opening most similar to the calculated values were selected and used for the docking of (A,E) 4P0, (B,F) 40P, (C,G) 41J, and (D,H) TxIA[A10L]. The disulfide bond at the tip of the C-loop is colored yellow.

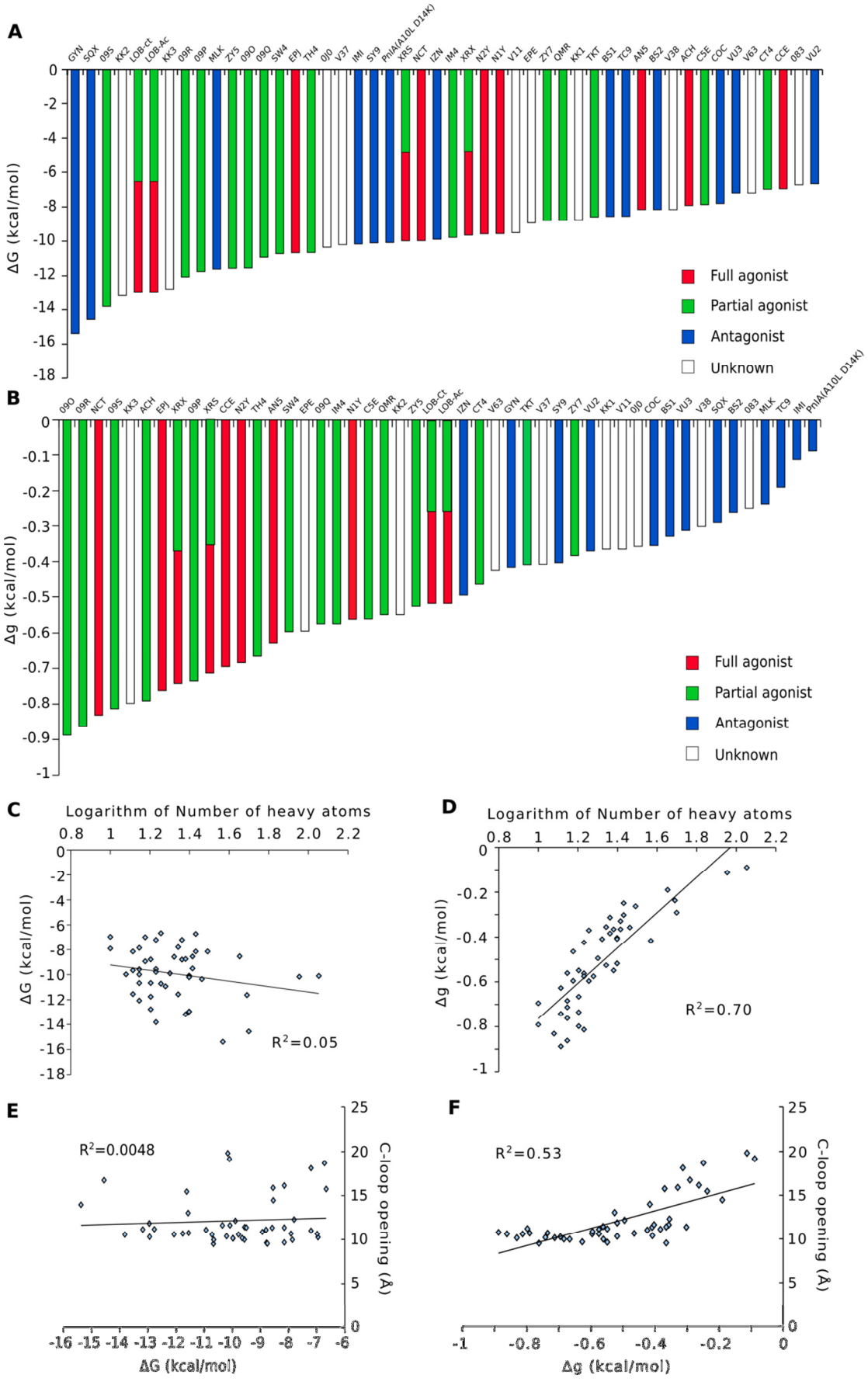
A
GYN SOX 09S KK2 LOB-Ct LOB-Ac KK3 09R 09P MLK ZY5 09O 09Q SW4 EPI TH4 0J0 V37 IMI SY9 PnIA(A10L D14K) XR5 NCT IZN IM4 XRX N2Y N1Y V11 EPE ZY7 QMR KK1 TKT BS1 TC9 AN5 BS2 V38 ACH C5E COC VU3 V63 CT4 CCE 083 VU2
ΔG (kcal/mol)
0 -2 -4 -6 -8 -10 -12 -14 -16 -18
Full agonist
Partial agonist
Antagonist
Unknown
B
09O 09R NCT 09S KK3 ACH EPI XRX 09P XR5 CCE N2Y TH4 AN5 SW4 EPE 09Q IM4 N1Y C5E QMR KK2 ZY5 LOB-Ct LOB-Ac IZN CT4 V63 GYN TKT V37 SY9 ZY7 VU2 KK1 V11 0J0 COC BS1 VU3 V38 SQX BS2 083 MLK TC9 IMI PnIA(A10L D14K)
Δg (kcal/mol)
0 -0.1 -0.2 -0.3 -0.4 -0.5 -0.6 -0.7 -0.8 -0.9 -1
Full agonist
Partial agonist
Antagonist
Unknown
C
Logarithm of Number of heavy atoms
0.8 1 1.2 1.4 1.6 1.8 2.0 2.2
ΔG (kcal/mol)
0 -2 -4 -6 -8 -10 -12 -14 -16 -18
R²=0.05
D
Logarithm of Number of heavy atoms
0.8 1 1.2 1.4 1.6 1.8 2.0 2.2
Δg (kcal/mol)
0 -0.2 -0.4 -0.6 -0.8 -1
R²=0.70
E
R²=0.0048
C-loop opening (Å)
25 20 15 10 5 0
-16 -15 -14 -13 -12 -11 -10 -9 -8 -7 -6
ΔG (kcal/mol)
F
R²=0.53
C-loop opening (Å)
25 20 15 10 5 0
-1 -0.8 -0.6 -0.4 -0.2 0
Δg (kcal/mol)

Figure 5. Correlation of the nAChR ligand binding free energy (ΔG) and ligand efficiency (Δg) to ligand size and C-loop opening. Ranking distribution of nAChR full agonists (red), partial agonists (green), antagonists (blue), and ligands with unknown property (white) based on their (A) ΔG and (B) Δg in order from low to high. The correlation coefficient score (R^2) for (C) ΔG and ligand size is 0.05, and (D) that for Δg and ligand size is 0.70. The R2 value for C-loop opening correlation with (E) ΔG and (F) Δg is 0.048 and 0.53, respectively. The ligand binding affinities and efficacies were determined using equations $\Delta G = -RT \ln K_d$ and $\Delta g = \Delta G/N_{\text{heavy atoms}}$ ($N_{\text{heavy atoms}}$, number of heavy atoms), respectively. The K_d values were determined using experimental approaches. In total, 61 compounds were docked into AChBP using ADT, while 59 nonpeptide compounds were selected for docking using MOE. MOE is poor at binding mode determination of peptides, and they were excluded in the docking set.

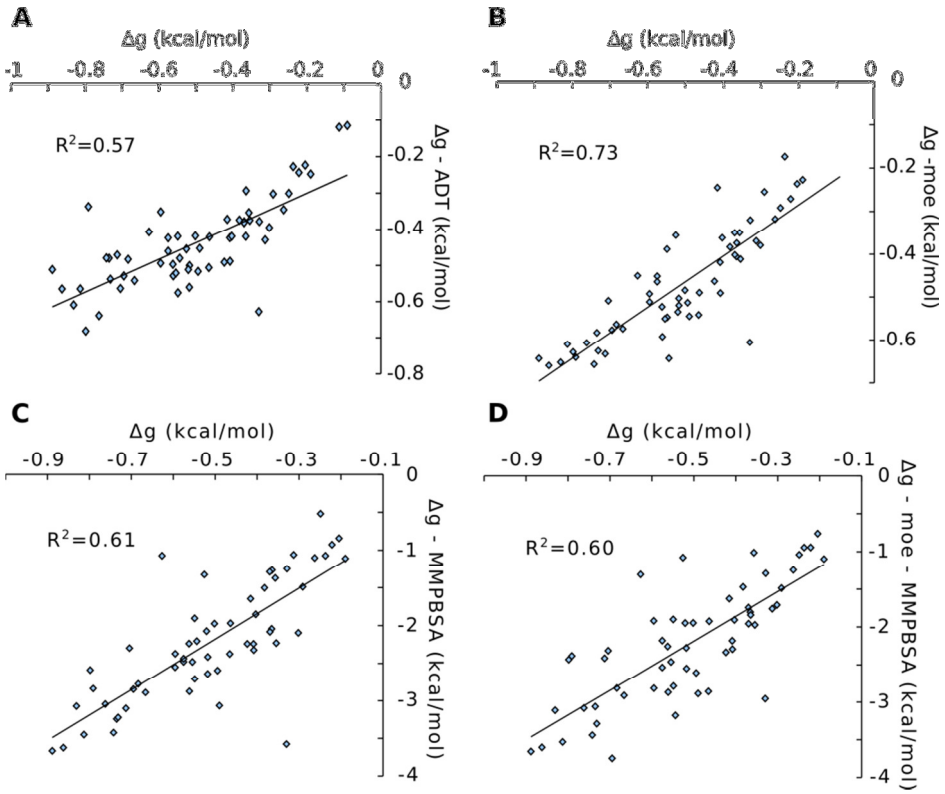

Figure 6. Correlation of computationally determined nAChR ligand efficiency (Δg) with those determined using experimental approaches. Ligand Δg calculated using (A) ADT, (B) MOE, and (C,D) MMPBSA method. For (C), MMPBSA calculation was directly performed on the crystal structures of AChBP bound with nAChR ligands, and in (D), MMPBSA was used to recalculate the binding affinities of the nAChR ligands docked using MOE. Ligand efficiency was calculated using the equation, $\Delta g = \Delta G/N_{\text{heavy atoms}}$ ($N_{\text{heavy atoms}}$, number of heavy atoms), where ΔG is the calculated binding affinity of the nAChR ligands using ADT, MOE, or MMPBSA.

Table 1. Comparison of computationally and experimentally determined C-loop opening of nAChR ligand-bound AChBP

ligand	number of heavy atoms	predicted C-loop opening[a] (Å)	PDB ID[b]	C-loop opening[c] (Å)	PDB ID[d]	C-loop opening[e] (Å)	RMSD[f] (Å)
4P0	12	10.22	3WIP	10.68	4ZJS	12.2	0.71
			3U8J	10.76			2.39
40P	51	14.51	2W8F	15.89	4XHE	17.67	0.52
			2XNT	15.75			0.78
41J	50	14.4	2BYR	15.46	4XK9	17.11	0.35
			2XYT	14.47			3.21
TxIA[A10L]	114	21.44	4BFQ	18.68	2UZ6	19.87	1.88
			2C9T	19.83			1.78

[a]Predicted C-loop opening using eq 3. [b]PDB ID of the two crystal structures of AChBP with similar C-loop opening to the predicted values selected for docking. [c]C-loop opening of the selected crystal structures. [d]PDB ID of the crystal structure bound with the docked ligand. [e]C-loop opening of the crystal structure bound with the docked ligand. [f]RMSD between the predicted ligand orientation and ligand orientation in the crystal structure of [d].